Research Square

Preprints are preliminary reports that have not undergone peer review.
They should not be considered conclusive, used to inform clinical practice,
or referenced by the media as validated information.

Physioxia-Induced Changes in Menstrual Blood-Derived Mesenchymal Stromal Cell Function and Extracellular Vesicle Cargo in a Fertility-Dependent Manner

Ilona Uzieliene

ilona.uzieliene@imcentras.lt

State Research Institute Centre for Innovative Medicine

Jolita Pachaleva

State Research Institute Centre for Innovative Medicine

Raminta Vaiciuleviciute

University College Dublin

Akvile Opolskiene

State Research Institute Centre for Innovative Medicine

Kieran Brennan

University College Dublin

Kristina Glusciukaite

State Research Institute Centre for Innovative Medicine

Daiva Bironaite

State Research Institute Centre for Innovative Medicine

Lina Piesiniene

Nanodiagnostika

Zaneta Kasilovskiene

MaxMeda

Margaret Mc Gee

University College Dublin

Eiva Bernotiene

State Research Institute Centre for Innovative Medicine

Research Article

Keywords: Menstrual blood-derived mesenchymal stromal cells, 5% O_2, oxygen tension, unexplained infertility, extracellular vesicles, proteomics.

Posted Date: November 18th, 2026

DOI: https://doi.org/10.21203/rs.3.rs-11338956/v1

License: This work is licensed under a Creative Commons Attribution 4.0 International License.
Read Full License

Additional Declarations: No competing interests reported.

Physioxia-Induced Changes in Menstrual Blood-Derived Mesenchymal Stromal Cell Function and Extracellular Vesicle Cargo in a Fertility-Dependent Manner

Ilona Uzieliene[1,3]*, Jolita Pachaleva[1], Raminta Vaiciuleviciute[2], Akvile Opolskiene[1], Kieran Brennan[2], Kristina Glusciukaite[1], Daiva Bironaite[1], Lina Piesiniene[3], Zaneta Kasilovskiene[4], Margaret Mc Gee[2], Eiva Bernotiene[1,5]*

[1] Department of Regenerative Medicine, Innovative Medicine Centre, Santariskiu St. 5, LT-08406 Vilnius, Lithuania
[2] Conway Institute of Biomolecular and Biomedical Research, University College Dublin, Belfield, Dublin 4, Ireland
[3] Nanodiagnostika, Ltd., Vilnius, Lithuania
[4] Medical Center "MAXMEDA", Vilnius, Lithuania
[5] Department of Chemistry and Bioengineering, Faculty of Fundamental Sciences, VILNIUS TECH, Vilnius, Lithuania

* Corresponding authors: Eiva Bernotiene, eiva.bernotiene@imcentras.lt; Ilona Uzieliene, ilona.uzieliene@imcentras.lt

Abstract

Background: Menstrual blood-derived mesenchymal stromal cells (MenSCs) originate from an endometrial environment in which oxygen tension is substantially lower than atmospheric culture conditions, yet the influence of oxygen tension on MenSC function and extracellular vesicle (EV) cargo remains insufficiently defined. We investigated MenSCs cultured at 5% O_2 and 21% O_2 to determine whether oxygen-dependent responses interact with fertility status, comparing cells derived from fertile (F) women and women with unexplained infertility (IF).

Methods: Functional characterization included viability, metabolic activity/proliferation, holographic migration and motility, glycolytic function, cell-cycle distribution, intracellular reactive oxygen species (ROS), surface phenotype and multiplex secretome analysis. Cellular and MenSC-EV proteomes were profiled by label-free mass spectrometry, with oxygen effects evaluated within fertility groups and fertility differences evaluated within each oxygen condition.

Results: MenSC viability was maintained under both oxygen conditions, whereas 5% O_2 promoted a more active functional/metabolic phenotype in the healthy/fertile MenSCs experiments. Across the fertility-comparison experiments, 5% O_2 revealed differences in cell-cycle progression and was associated with a distinct redox, phenotypic and secretory response in IF MenSCs. Proteomic analysis supported oxygen-dependent remodeling of metabolism/redox regulation, Ca^{2+} signaling, cytoskeletal/ECM organization and intracellular signaling. EV proteomics showed that oxygen tension also altered exported protein cargo and that this response differed by fertility status. Notably, F MenSCs EVs at 5% O_2 were enriched in proteins related to RNA/protein processing and Ca^{2+} homeostasis, whereas IF MenSCs EVs showed a distinct mitochondrial/metabolic response and greater representation of redox and signaling proteins at 21% O_2. Integrated cell-EV analysis identified convergent pathway-level changes, including metabolic/redox, Ca^{2+}, ECM/cytoskeletal and growth-signaling networks.

Conclusions: These findings identify oxygen tension as an important modulator of the MenSC phenotype, with responses that vary according to fertility status. They also highlight MenSC-derived EV cargo as a promising candidate biomarker of fertility-associated adaptation to oxygen tension, warranting further validation in larger and independent cohorts.

Keywords

Menstrual blood-derived mesenchymal stromal cells; 5% O_2; oxygen tension; unexplained infertility; extracellular vesicles; proteomics.

1. Background

Menstrual blood is a non-invasively accessible biological material containing endometrial stromal cells, immune cells, soluble mediators and extracellular vesicles (EVs) (1). Menstrual blood-derived mesenchymal stromal cells (MenSCs) are particularly attractive for reproductive and regenerative research because they can be obtained repeatedly without an invasive biopsy and exhibit characteristic mesenchymal stromal cell properties, high proliferative capacity, low immunogenicity, and a biologically active secretome (2)(3). MenSCs have consequently gained interest both as a model of endometrial stromal biology and as a potential source of regenerative cell- and EV-based products. Previous work from our group has demonstrated that MenSCs and MenSC-derived EVs contain fertility-associated proteomic signatures, with alterations in pathways related to cellular adhesion, immune regulation, fibrosis and metabolism in women with unexplained infertility (4). In parallel, EVs isolated directly from menstrual blood serum were shown to carry infertility-associated molecular signatures involving cell adhesion, immune responses, apoptosis, oxidative stress and lipid metabolism, further supporting menstrual blood as a source of molecular information relevant to endometrial and reproductive function (5).

An important but frequently underestimated determinant of stromal-cell phenotype is oxygen tension. Conventional *in vitro* culture is commonly performed at approximately 21% O_2, although oxygen concentrations within most tissues are substantially lower. The term “physioxia” is therefore increasingly used to describe oxygen levels that more closely approximate the physiological microenvironment of a particular tissue, rather than defining atmospheric oxygen as physiological “normoxia”. Studies across mesenchymal stromal cell populations have demonstrated that culture under physioxic conditions can influence proliferation, differentiation, metabolic programming and cellular stress responses, in part through stabilization of hypoxia-inducible factor signaling and adaptation of mitochondrial and glycolytic metabolism (6).

The endometrium is especially relevant in this context because its oxygen environment is dynamic. Cyclic vascular remodeling, vasoconstriction, menstrual shedding, tissue breakdown and rapid subsequent repair expose endometrial cells to changing oxygen availability. Such fluctuations are biologically linked to cellular metabolism, angiogenesis, inflammation and tissue regeneration, all of which are central to normal endometrial function and implantation (7). Thus, maintaining endometrial stromal cells continuously at atmospheric oxygen may not fully reproduce their physiological state.

In the present study, 5% O_2 was selected as a practically achievable physioxic culture condition, while 21% O_2 represents conventional atmospheric culture. This distinction is important because physioxia is not necessarily equivalent to pathological hypoxia, rather, it represents a lower oxygen environment that may more closely reflect the physiological niche encountered by stromal cells *in vivo*. Studies of MSCs from several tissue sources have shown that exposure to approximately 2–5% O_2 can preserve viability, enhance proliferation or colony-forming capacity and alter migratory, metabolic, angiogenic and differentiation-associated functions (8)(9).

EV composition is dynamically influenced by the physiological state and microenvironment of the parental cells. In MSCs, reduced oxygen availability can modify EV protein and nucleic-acid cargo, with corresponding changes in their biological activity. MenSC-derived EVs are similarly responsive to oxygen conditions, suggesting that physioxia may influence not only MenSCs function but also the molecular information conveyed by their EVs (8).

This may be particularly relevant to IF, a heterogeneous condition associated with altered endometrial receptivity, immune regulation, oxidative stress and metabolism. Our previous proteomic studies demonstrated fertility-associated differences in MenSCs, MenSC-EVs and menstrual blood EVs, compared to IF samples, particularly in pathways related to metabolism, adhesion, immune regulation, fibrosis and oxidative stress (4)(5). MenSC-EVs also exhibit biological activity in recipient cells and tissues, supporting their role as functional mediators of intercellular communication (10). However, whether physioxia, compared to normoxia, differentially affects MenSC function and EV cargo according to fertility status, remains unknown.

The aim of the present study was to determine how culture under physioxic conditions (5% O_2), compared with conventional atmospheric oxygen (21% O_2), affects the functional, metabolic, phenotypic, secretory and proteomic characteristics of MenSCs and their EV cargo, and to establish whether these oxygen-dependent responses differ between MenSCs derived from fertile (F) and infertile (IF) women, experiencing unexplained IF.

The study was designed in two complementary stages. First, we characterized the effect of 5% O_2 on fundamental MenSC properties, including viability, proliferation/metabolic activity, migration, motility and glycolytic function. Second, we investigated fertility-dependent oxygen adaptation by comparing cell-cycle distribution, intracellular reactive oxygen species, surface phenotype and secretome together with cellular and EV proteomic profiles in F and IF donor-derived MenSCs cultured at 5% O_2 and 21% O_2 conditions.

To our knowledge, no prior study has examined whether MenSCs and their EV cargo itself differ according to fertility status and 5% O_2 and 21% O_2 cultivation conditions. We therefore hypothesize that MenSCs derived from women with proven fertility and those with unexplained IF will exhibit distinct adaptive responses to reduced-oxygen culture conditions, detectable at the levels of cellular metabolism and redox state, cell-cycle dynamics, surface phenotype, and EV protein cargo, rather than assuming that physioxia will induce a uniform or superior functional phenotype in either group.

2. Methods

2.1 The aim, study design and donor groups

The aim of this study was to investigate the effects of physiologically relevant oxygen tension (5% O_2), compared with conventional atmospheric oxygen (21% O_2), on the functional, phenotypic, and molecular characteristics of MenSCs and their EVs. Particular emphasis was placed on identifying oxygen-dependent responses associated with donor fertility status by comparing MenSCs derived from F women and women with IF.

Menstrual blood-derived MenSCs from F women (n=8) and women with IF (n=5) were used in this study. F participants (aged 27-40) were defined by a history of natural conception and delivery of at least one healthy child without pregnancy loss. IF participants (aged 32-42) met clinical criteria for unexplained infertility, including inability to conceive after at least 12 months of regular unprotected intercourse, regular menstrual cycles, absence of identified gynecological or systemic causes, and a partner with normal semen-analysis parameters. Participant selection and menstrual blood collection followed the framework used in our previous MenSC studies. The number of biological donors varied between assays according to sample availability and is stated in the corresponding figure legends.

2.2 MenSC isolation and culture

MenSCs were isolated from menstrual blood as discussed previously (10)(11)(12). Briefly, the blood sample was collected by donors using silicon cups (iCare, Wuhan, China) and MenSCs isolation was performed using the Ficoll-Paque PLUS (Stem Cell Technologies, Cologne, Germany) density-gradient centrifugation (40 min, 400 *g*), then washed two times in phosphate-buffered saline (PBS) (Sigma Aldrich, Taufkirchen, Germany), then centrifuged (10 min, 400 *g*). The mononuclear-cell fraction was collected and cells were expanded in DMEM/F12 (Merck Millipore, Darmstadt, Germany) supplemented with 10% fetal bovine serum (FBS) (Merck Millipore, Darmstadt, Germany) and 1% penicillin/streptomycin (PS) (Gibco, Thermo Fisher Scientific, Waltham, MA, USA) at 37 °C and 5% CO_2. Medium was changed twice a week, and after cells reached confluence of ~ 80%, they were detached using a 0.25% solution of trypsin-EDTA (Gibco, Thermo Fisher Scientific, Waltham, MA, USA), counted and sub-cultured. Early-passage cells (P=1-3) were used to minimize culture-associated phenotypic drift. MenSCs identity and mesenchymal phenotype had been established in our previous studies by plastic adherence, surface-marker analysis and differentiation capacity (12).

2.3 Oxygen exposure

For experimental comparisons, MenSCs were cultured at either 5% O_2 (physioxia) or 21% O_2 (normoxia) while temperature (37 °C), CO_2 (5%) and other culture conditions were kept constant. Biospherix hypoxia chamber was used for physioxic environment. Cells and medium were equilibrated and maintained under the assigned oxygen condition throughout the experimental period. In the manuscript, oxygen conditions are reported numerically as 5% O_2 and 21% O_2 to avoid ambiguity associated with the terms physioxia, hypoxia and normoxia.

2.4 MenSC viability and metabolic activity/proliferation

Cell viability was assessed by seeding the MenSCs into 12-well plates, 20,000 cells/well, under both oxygen conditions. The next 1,3,5 and 7 days the cell metabolic activity/proliferation was assessed using the Alamar Blue assay (Gibco, Thermo Fisher Scientific, Waltham, MA, USA) according to the manufacturer's instructions. Absorbance was measured at 570 nm using a SpectraMax i3 (Thermo Fisher Scientific, Waltham, MA, USA) microplate reader. After 7 days, Live/Dead (Sigma Aldrich, Taufkirchen, Germany) fluorescence staining was used and representative viable/dead-cell images were acquired under both oxygen conditions using EVOS M7000 Imaging System (Thermo Fisher Scientific, Waltham, MA, USA). Absorbance values were background corrected and compared between oxygen conditions. Six biological MenSC samples were included in the analysis.

2.5 Holographic migration and motility analysis

Cell migration and motility speed were assessed by digital holographic imaging using the HoloMonitor system (PhiAB, Sweden) and the Single Cell Tracking protocol. MenSCs were cultured under physioxic/normoxic conditions for 7 days, then detached and seeded into 6-well plates at a density of 10,000 cells/well and cultured overnight under the respective oxygen conditions (5% O_2

or 21% O_2). The following day, plates were equipped with HoloLids and transferred to the HoloMonitor for continuous live-cell imaging for 24 h at 37 °C and 5% CO_2. Due to the configuration of the imaging system, holographic recording was performed under 21% O_2. Therefore, this experiment assessed the effect of prior culture under 5% O_2 or 21% O_2 on subsequent cell migration and motility rather than continuous migration under the respective oxygen conditions. For each well, 6–8 representative positions were monitored, with images acquired every 2 h. Individual cells were identified and tracked using HoloSuit software, and migration distance and motility speed were extracted from the resulting single-cell trajectories. The analysis included two independent donor-derived MenSC preparations (n = 2).

2.6 Seahorse glycolytic analysis

Glycolytic function of MenSCs previously cultured under 5% O_2 and 21% O_2 for 7 days was assessed using a Seahorse XFp Analyzer (Agilent Technologies, Santa Clara, CA, USA) together with the Seahorse XFp Glycolysis Stress Test Kit (Agilent Technologies, Cat. No. 103017-100), according to the manufacturer's protocol. MenSCs from three independent donors (n = 3) were maintained under the respective oxygen conditions before the assay and seeded into Seahorse XFp cell-culture miniplates at 10,000 cells/well. Prior to extracellular flux measurement, the culture medium was replaced with Seahorse XF assay medium supplemented with glutamine, and cells from both oxygen conditions were equilibrated for 1 h at 37 °C in a CO_2-free incubator under atmospheric oxygen. Thus, cells previously maintained at 5% O_2 underwent reoxygenation during assay preparation and extracellular flux measurement, and the Seahorse experiment reflects metabolic characteristics following prior oxygen exposure rather than measurements performed continuously at 5% O_2.

Extracellular acidification rate (ECAR) was recorded at baseline and following sequential injection of glucose, oligomycin and 2-deoxy-D-glucose (2-DG). These measurements were used to determine non-glycolytic acidification, glycolysis, glycolytic capacity and glycolytic reserve.

Following the assay, cells were fixed with 4% paraformaldehyde and stained with DAPI. Cell nuclei were imaged and counted using the EVOS M7000 Imaging System, and ECAR measurements were normalized to cell number. Data were processed using Seahorse Wave software (Agilent Technologies).

2.7 Cell-cycle analysis

MenSCs were cultured under 5% O_2 or 21% O_2 for 7 days to approximately 70% confluence. Cell-cycle distribution was assessed using the CellCycleFlowEx kit (Exbio, ED7069) according to the manufacturer's protocol. Samples were measured using a Luminex Guava (Merck Millipore, Darmstadt, Germany) flow cytometer under 21% O_2 and analyzed using FlowJo v11 software (BD Biosciences, Ashland, OR, USA). The proportions of cells in G1, S and G2M phases were quantified in percentage.

2.8 Intracellular ROS

Intracellular reactive oxygen species (ROS) were quantified using the Muse Oxidative Stress Kit (Cytek Biosciences) according to the manufacturer's instructions. The assay is based on oxidation of dihydroethidium and detection of the resulting fluorescence. Approximately 10,000 cells were

analyzed per measurement under 21% O_2. F and IF MenSCs were compared after incubation under 5% O_2 and 21% O_2 for 7 days. The analysis included at least three independent donor-derived cell preparations per group.

2.9 Surface-marker analysis

MenSC surface phenotype was evaluated by flow cytometry in F (n = 5-14) and IF (n = 3-7) donor-derived cell preparations cultured under 5% O_2 and 21% O_2. Following culture under the respective oxygen conditions, MenSCs were detached, washed with PBS supplemented with 1% bovine serum albumin (BSA; Sigma-Aldrich, USA), and centrifuged at 500 *g* for 5 min. Cells were subsequently divided into aliquots of approximately 100,000 cells per staining condition.

Immunostaining was performed in PBS containing 1% BSA using fluorescently labeled (FITC/PE) antibodies against the selected human cell-surface cluster of differentiation (CD) antigens: CD9, CD10, CD13, CD56, CD62L, CD63, CD73, CD90, CD105, Notch1. Antibodies were added according to the manufacturers' recommendations, and cells were incubated for 30 min at 4 °C in the dark. Following incubation, cells were washed to remove unbound antibodies and resuspended in PBS for flow cytometric analysis. Unstained cells were used as controls to establish positivity gates and distinguish specific autofluorescence signal.

For each sample, 10,000 events were acquired using a Luminex Guava flow cytometer under 21% O_2. Cell populations were identified based on forward- and side-scatter characteristics, and cellular debris was excluded prior to analysis of marker expression. Data were analyzed using FlowJo v11 software. Surface antigen expression was quantified as the percentage of positive cells and/or median fluorescence intensity (MFI), as appropriate for each marker, and compared between MenSCs cultured under 5% O_2 and 21% O_2 and between F and IF donor groups.

2.10 Multiplex secretome analysis

Conditioned media were collected from F and IF MenSCs cultured under 5% O_2 and 21% O_2. Human Cytokine/Chemokine/Growth Factor Panel Kit (Invitrogen, Thermo Fisher Scientific, Waltham, MA, USA) was used according to manufacturer's instructions. The supernatants were used without dilution. The analysis was performed using a Luminex 200 instrument and a panel of 45 human cytokines/chemokines and growth factors were measured. Sample numbers varied between analytes according to sample availability and detection above the assay range (n=3-8). Analytes below the reliable detection limit were excluded from interpretation.

2.11 EV collection, isolation and characterization

For EV collection, confluent MenSCs cultures were washed and conditioned in serum-free DMEM/F12 for 48 h, following our previously published MenSC-EV workflow. Conditioned medium was cleared of cells and debris by centrifugation and EVs were isolated by ultracentrifugation followed by iodixanol density-gradient purification as previously described (4). EV identity and purity had been established for this workflow according to MISEV principles using complementary approaches including transmission electron microscopy, EV-associated proteins (e.g., CD63 and TSG101), assessment of non-EV contaminants, and tetraspanins analysis (CD9, CD63 and CD81) by flow cytometry (4)(5). Because the present study focuses on oxygen-dependent EV proteomic cargo, detailed validation of the established isolation workflow is referenced to our

prior publications rather than repeated in full. The same isolation and processing strategy was applied across comparison groups.

2.12 MenSCs and EV proteomics

Cell lysates and purified MenSC-EVs were subjected to label-free mass-spectrometry proteomics. Proteins were reduced, alkylated, digested with trypsin and analyzed using a Bruker timsTOF Pro mass spectrometer coupled to an Evosep One liquid-chromatography system, consistent with our previous proteomic workflow. Raw spectra were searched against the reviewed Homo sapiens UniProt/Swiss-Prot database using MaxQuant (version 2.0.1.0) with TIMS-DDA settings. Peptide/protein identification was controlled at a database-search FDR of 1%, and normalized label-free quantification (LFQ) intensities were used for comparative analyses.

2.13 Proteomic preprocessing and statistical analysis

For the oxygen-response proteomics, technical mass-spectrometry replicates were averaged within each biological donor before statistical testing. Zero LFQ entries representing non-detection were treated as missing rather than true zero abundance. Obvious contaminant and reverse-sequence entries were excluded. Oxygen effects (5% O_2 vs 21% O_2) were evaluated as paired comparisons within donors, while fertile-versus-infertile contrasts within each oxygen condition were evaluated between biological donor groups. An oxygen × fertility-status interaction was estimated from the donor-level oxygen response (5% O_2 minus 21% O_2). Benjamini-Hochberg false-discovery-rate correction was applied separately within each contrast. For visualization, volcano plots display $\log_2$ fold change versus $-\log_{10}(p)$, and proteins with nominal p<0.05 and $|\log_2 FC| \geq 1$ were highlighted as exploratory candidates. To ensure that conclusions reflect biologically coherent patterns rather than isolated data points, individual protein findings, particularly within the cellular proteomics dataset, were interpreted as exploratory candidates unless supported by FDR correction and/or convergent pathway-level evidence.

2.14 Bioinformatics analysis

Volcano plots were generated using SRplot. Functional enrichment was evaluated using ShinyGO and comparable GO/KEGG pathway tools with Homo sapiens as the reference species. Gene lists were analyzed separately according to direction of change, and the background was restricted to proteins tested/detected in the corresponding contrast were supported by the software. Heatmaps were generated from donor-level $\log_2$ LFQ intensities with row-wise scaling to visualize relative abundance patterns across F and IF donors at 5% O_2 and 21% O_2. Pathway interpretation prioritized coherent biological themes rather than isolated nominally significant proteins.

2.15 General statistical analysis

Data are presented as mean ± standard deviation (SD) unless otherwise indicated, and the number of independent biological donors (n) is specified for each experiment. For experiments comparing MenSCs according to both oxygen condition (5% O_2 vs 21% O_2) and fertility status (F vs IF), two-way analysis of variance (ANOVA) was used to evaluate the effects of oxygen condition, fertility status, and their interaction, followed by appropriate multiple-comparison post hoc tests.

7

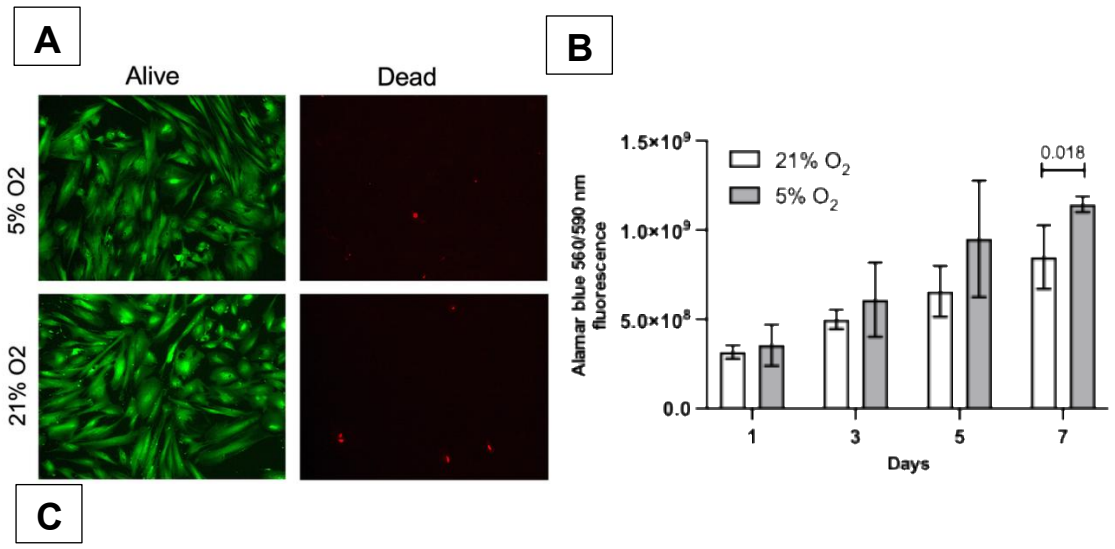
When only two experimental conditions were compared, paired statistical tests were applied when the same donor was analyzed under both oxygen conditions, whereas unpaired tests were used for comparisons between independent donor groups. Statistical significance was considered at $p < 0.05$. Statistical analyses were performed using GraphPad Prism v10, (GraphPad Software, Boston, MA, USA).

3. Results

3.1. Physioxia reprograms the functional and metabolic state of F MenSCs

MenSCs remained predominantly viable under both oxygen conditions, with no apparent detrimental effect of culture at 5% O_2 compared with 21% O_2 (Fig. 1A). Metabolic activity/proliferation was significantly increased at 5% O_2, as demonstrated by a higher Alamar Blue signal at day 7 compared with 21% O_2 ($P = 0.018$; Fig. 1B). Holographic single-cell tracking suggested lower migration distance and motility speed in MenSCs previously cultured at 5% O_2 compared with 21% O_2 (Fig. 1C). Given the small number of biological donors ($n = 2$) and the subsequent imaging of both groups under 21% O_2, these findings should be considered preliminary and interpreted as an effect of prior oxygen exposure rather than continuous migration under physioxia.

Seahorse analysis demonstrated a pronounced metabolic response following prior culture at 5% O_2. MenSCs previously cultured at 5% O_2 exhibited significantly increased basal glycolysis ($P = 0.0002$), glycolysis ($P = 0.0016$) and glycolytic capacity ($P = 0.0096$) compared with cells cultured at 21% O_2 (Fig. 1D), whereas glycolytic reserve was lower at 5% O_2. Together, these results indicate that culture at 5% O_2 promotes a more glycolytically active metabolic state and increases metabolic activity/proliferation without compromising cell viability. In contrast, migration and motility did not show a corresponding increase, indicating that the response to reduced oxygen is function-specific rather than uniformly stimulatory.



8

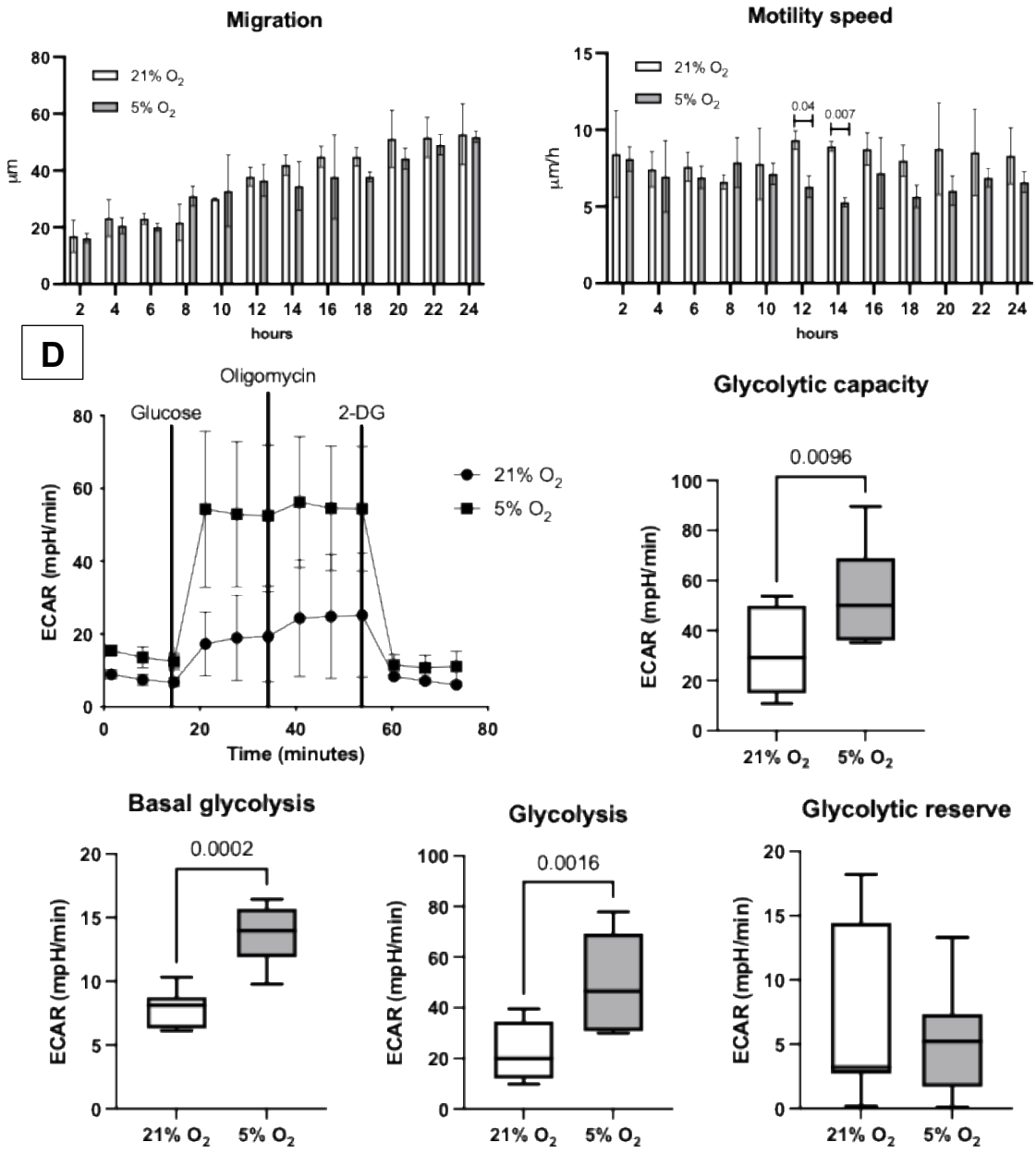


Figure 1. Functional and metabolic response of MenSCs to 5% O_2 and 21% O_2. (A) Representative Live/Dead images show cell viability under both oxygen conditions (Calcein-AM (green live cells) and ethidium homodimer-1 (red dead cells)). x100 magnification. (B) Quantitative panels show Alamar Blue metabolic activity/proliferation (n=6). (C) Holographic single-cell migration and motility speed measured using the PhiAB system (n=2), and (D) glycolytic function measured using an Agilent Seahorse extracellular flux analyzer (n=3), presenting ECAR glycolytic capacity, basal glycolysis, total glycolysis and glycolytic reserve. Data are presented as indicated in individual panels; statistical annotations denote the comparisons shown.

3.2. Fertility-associated MenSC responses to 5% O_2 and 21% O_2

3.2.1. Cell-cycle distribution

Cell-cycle distribution differed according to both oxygen condition and fertility status (Fig. 2). F MenSCs, cultured at 5% O_2 significantly increased the proportion of cells in the G2M phase compared with 21% O_2 ($P < 0.0001$). In contrast, IF MenSCs responded to 5% O_2 with a significant increase in the proportion of cells in S phase ($P < 0.0001$), indicating a distinct cell-cycle response to physioxia between the two donor groups.

9

Direct comparison of F and IF MenSCs further demonstrated that fertility-associated differences were dependent on oxygen conditions, i.e. at 21% O_2, IF MenSCs exhibited a significantly higher proportion of cells in G2M compared with F MenSCs ($P = 0.0007$). Under 5% O_2, however, this relationship was reversed, with IF MenSCs showing a significantly lower proportion of cells in G2M than F MenSCs ($P < 0.0001$). Together, these results indicate that physioxia differentially modulates cell-cycle progression in F and IF MenSCs, promoting G2M accumulation in F cells while favoring S-phase representation in IF cells. The F MenSCs accumulated more in G2M under physioxic condition, while IF MenSCs – under normoxic.

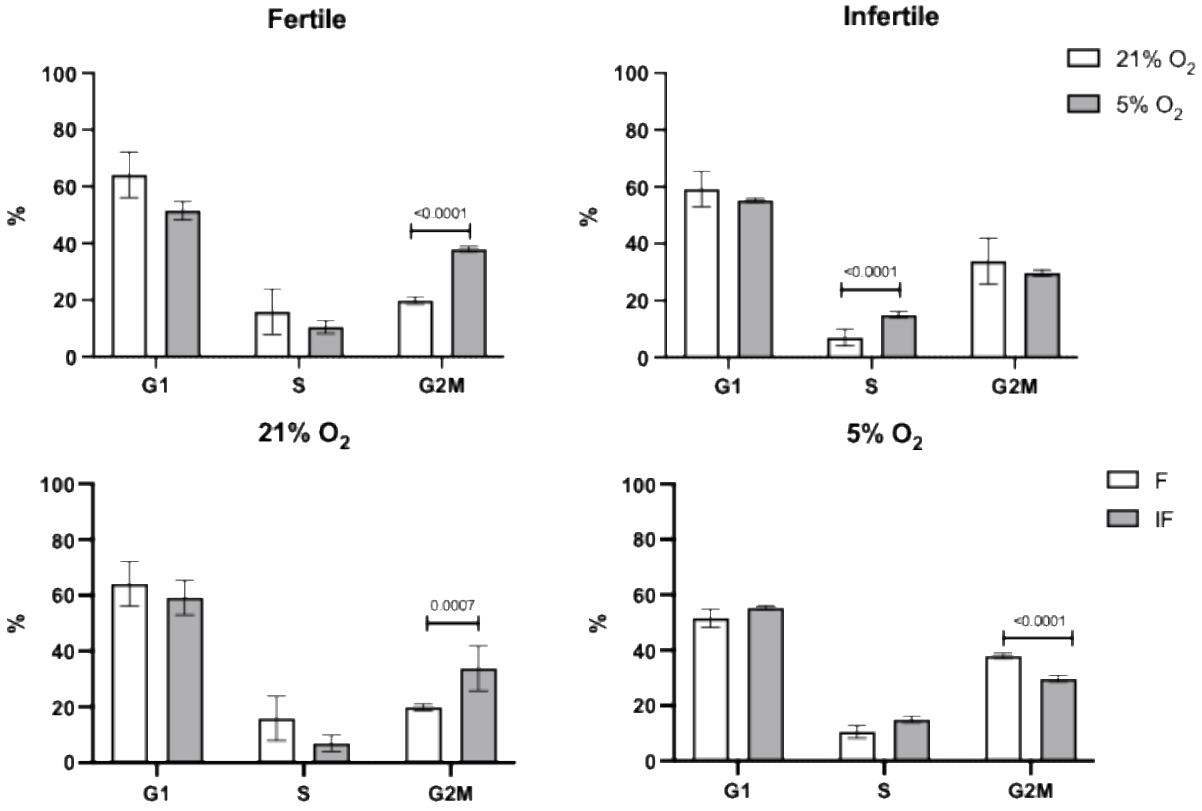


Figure 2. Cell-cycle distribution of F (n=3) and IF (n=3) MenSCs cultured at 5% O_2 and 21% O_2. Cells were cultured for 7 days and the proportions in G1, S and G2M phases were quantified using flow cytometry and calculated using FlowJo v11.

3.2.2. Intracellular ROS

Intracellular ROS levels were quantified in F and IF MenSCs cultured under 5% O_2 and 21% O_2 using the Muse Oxidative Stress assay. Under conventional 21% O_2 conditions, IF MenSCs exhibited markedly higher intracellular ROS levels than F MenSCs ($P < 0.0001$), indicating a pronounced fertility-associated difference in cellular redox status (Fig. 3).

Exposure to 5% O_2 significantly reduced intracellular ROS levels in both F and IF MenSCs, although the effect was considerably stronger in the IF group ($P = 0.0410$ for F MenSCs and $P < 0.0001$ for IF MenSCs). Therefore, the marked difference in ROS levels between F and IF MenSCs observed at 21% O_2 was substantially attenuated under 5% O_2 conditions.

These findings suggest that physioxia partially normalizes the elevated oxidative state in both cell types, with a more pronounced effect on IF MenSCs. The fertility-associated ROS phenotype is more clearly detectable under conventional atmospheric oxygen conditions than under physioxia.

10

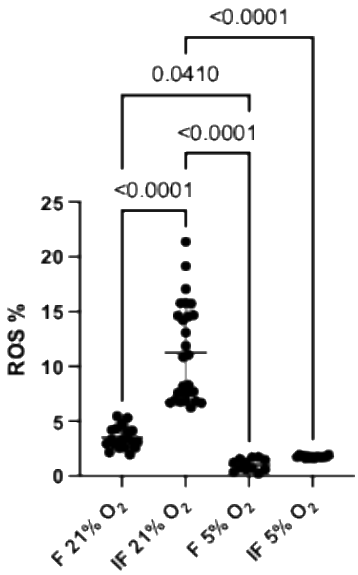


Figure 3. Intracellular ROS in F (n=3) and IF (n=3) MenSCs cultured at 5% O_2 and 21% O_2. ROS-positive cells were quantified using the Muse Oxidative Stress Kit. Data are shown as mean ± SD from at least three independent donor-derived cell preparations per group.

3.2.3. Surface phenotype

Surface-marker analysis demonstrated that MenSCs retained their characteristic mesenchymal stromal phenotype under both oxygen conditions, although the levels of selected surface markers were modulated by oxygen tension and fertility status (Fig. 4). In F MenSCs, culture under physioxic conditions (5% O_2) resulted in significantly higher levels of CD9 (tetraspanin), ($P = 0.007$) and CD105 (endoglin) ($P = 0.005$) compared with 21% O_2. CD9 is involved in cell adhesion, migration, and extracellular vesicle release, whereas CD105 is a characteristic mesenchymal stromal cell marker and functions as a co-receptor for transforming growth factor-β (TGF-β), contributing to the regulation of cellular responses involved in proliferation, migration, angiogenesis, and tissue remodeling (13)(14). The increased levels of CD9 and CD105 under 5% O_2 indicate that physiologically relevant oxygen conditions selectively modify surface proteins associated with membrane organization, cell adhesion, and TGF-β-related signaling in F MenSCs.

In contrast, CD73 (Ecto-5'-nucleotidase) level in F MenSCs was significantly higher under conventional 21% O_2 condition than at 5% O_2 ($P = 0.03$). CD73 converts extracellular AMP into adenosine, which is a powerful immunosuppressive and anti-inflammatory molecule (15). The higher CD73 level observed at 21% O_2 suggests that oxygen tension may influence the adenosinergic phenotype of F MenSCs; however, the functional consequences of this difference for their immunomodulatory activity remain to be determined.

In IF MenSCs, the response to oxygen tension was less pronounced, with CD9 being the only marker significantly increased under 5% O_2 compared with 21% O_2 ($P = 0.04$). Together, these data indicate that 5% O_2 selectively modifies the MenSC surface phenotype, with some responses, particularly the increase in CD9, shared between F and IF MenSCs.

Direct comparison of F and IF MenSCs further revealed that fertility-associated phenotypic differences depended on the oxygen environment: under 21% O_2, CD13 (a specific cell-surface enzyme, also known as Aminopeptidase N) was significantly higher in IF MenSCs compared with F MenSCs ($P = 0.00017$), whereas no significant fertility-associated differences were detected for the other analyzed markers. The higher CD13 level in IF MenSCs at 21% O_2 indicates a fertility-

11

associated difference in surface phenotype under conventional atmospheric oxygen conditions, although the functional significance of this difference remains to be determined.

In addition, under 5% O_2 culture condition CD105 level was significantly higher in F than in IF MenSCs (P = 0.02). This difference was consistent with the pronounced increase in CD105 observed in F MenSCs following exposure to 5% O_2, whereas a comparable response was not detected in IF cells. The higher CD105 level in F compared with IF MenSCs at 5% O_2 further indicates that oxygen-dependent regulation of the MenSC surface phenotype differs according to fertility status.

These findings indicate that oxygen tension selectively modifies the MenSCs surface phenotype and that this phenotypic adaptation differs according to fertility status. The changes were restricted to specific markers rather than reflecting a general alteration or loss of mesenchymal stromal identity. In particular, the differential regulation of CD105 under 5% O_2 suggests a distinct response of F and IF MenSCs to a physiologically relevant oxygen environment, providing further evidence that fertility-associated MenSC phenotype may become differently manifested depending on culture oxygen tension.

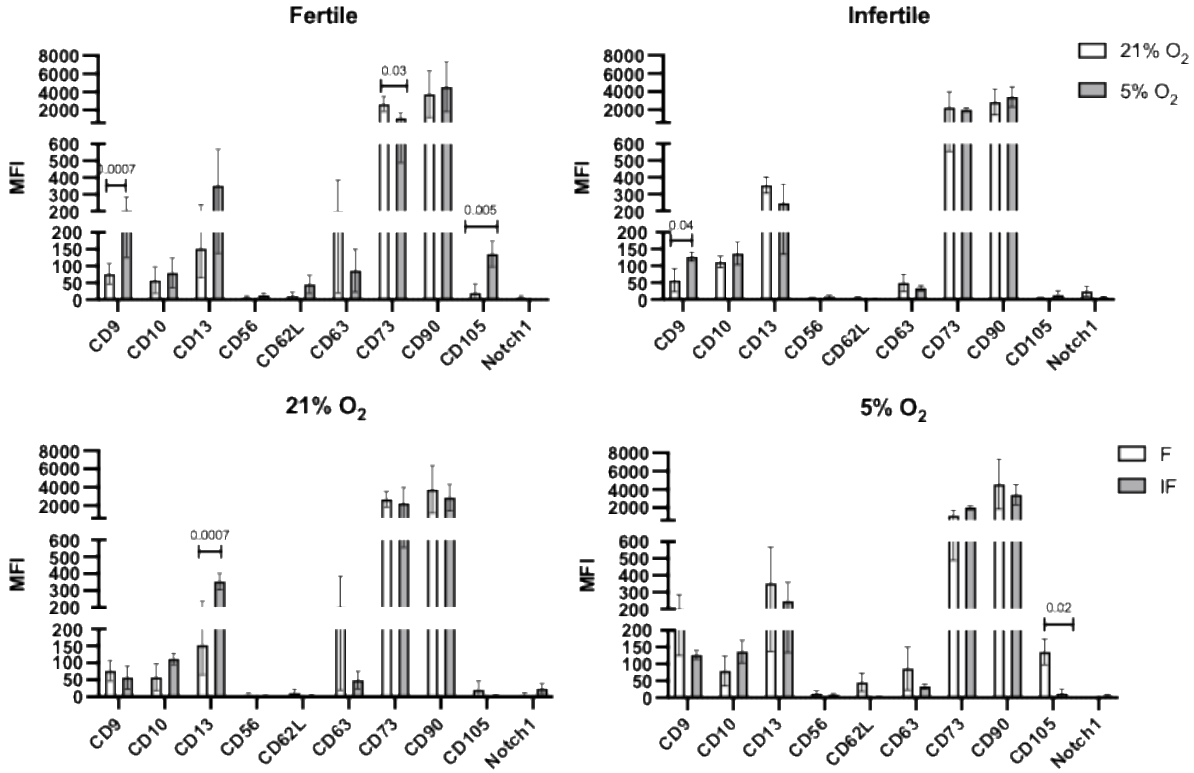


Figure 4. Surface phenotype of F and IF MenSCs cultured at 5% O_2 (F n=4; IF n=3) and 21% O_2 (F n=14; IF n=7). Selected surface markers were quantified by flow cytometry in F and IF donor-derived MenSCs. Results are presented as median fluorescence intensity (MFI).

3.2.4. **Secretome profile**

Multiplex analysis was performed to characterize the soluble secretory profile of F and IF MenSCs cultured under 5% O_2 and 21% O_2 (Fig. 5). A broad panel of cytokines, chemokines and growth factors was measured, however, only factors that were consistently detectable and/or demonstrated relevant differences between oxygen conditions or fertility groups are presented. Several growth and angiogenesis-associated factors, including Fibroblast Growth Factor 2 (FGF-2), Hepatocyte Growth Factor (HGF) and Vascular Endothelial Growth Factor (VEGF-A), were detected

12

in MenSC-conditioned media but did not differ significantly according to oxygen condition or fertility status. Similarly, interleukins 6 and 9 (IL-6 and IL-9) showed no statistically significant quantitative differences between the analyzed groups.

In contrast, SDF-1 (stromal cell-derived factor 1) was significantly increased in conditioned medium from F MenSCs cultured under 5% O_2 compared with 21% O_2 ($P = 0.048$), indicating enhanced secretion of this chemotactic factor in response to physioxia. Also known as CXCL12, SDF-1 is a small signaling protein (chemokine) that regulates cell migration, tissue repair, and stem cell homing through binding to receptors such as CXCR4 (16).

Conversely, MCP-1 (monocyte chemoattractant protein-1) secretion was significantly reduced under 5% O_2 in both F ($P = 0.0288$) and IF ($P = 0.0444$) MenSCs, suggesting a shared oxygen-dependent suppression of MCP-1 secretion irrespective of fertility status. MCP-1 is a chemokine involved in recruiting immune cells to sites of tissue damage or infection (17). Thus, reduced MCP-1 secretion may indicate decreased inflammatory signaling under physioxia.

An additional distinction was observed for factors present at very low concentrations or close to the assay detection limit: in conditioned medium from IF MenSCs cultured at 21% O_2 were detectable interleukin 6 (IL-6), leukemia inhibitory factor (LIF), and placental growth factor-1 (PlGF-1), whereas under 5% O_2 and in the corresponding F MenSCs cultures, these factors were either undetectable or present only at trace levels. IL-6 is involved in inflammation, immune responses, and cell signaling, while LIF plays an important role in stem cell self-renewal and embryo implantation (18)(19). PlGF-1 is involved in the regulation of angiogenesis and blood vessel growth (20). The higher levels ($P = 0.0393$) of these factors in IF MenSCs under 21% O_2 suggest that oxygen availability may cause some inflammation and affect the paracrine communication of IF MenSCs with their extracellular environment. Although these low-abundance measurements should be interpreted cautiously and were not subjected to definitive quantitative comparisons, their selective detection in IF MenSCs under atmospheric oxygen suggests that 21% O_2 may promote or reveal a distinct secretory state in these cells.

Overall, the secretome data do not indicate a generalized increase or suppression of MenSCs cytokine secretion in response to physioxia. Instead, lowering oxygen tension from 21% to 5% O_2 selectively remodeled the paracrine profile, characterized most clearly by increased SDF-1 secretion in F MenSCs and reduced MCP-1 secretion in both F and IF cells. The findings suggest that oxygen tension is an important regulator of MenSC function and extracellular communication, with distinct adaptive responses in MenSCs derived from women with proven fertility and unexplained infertility.

13

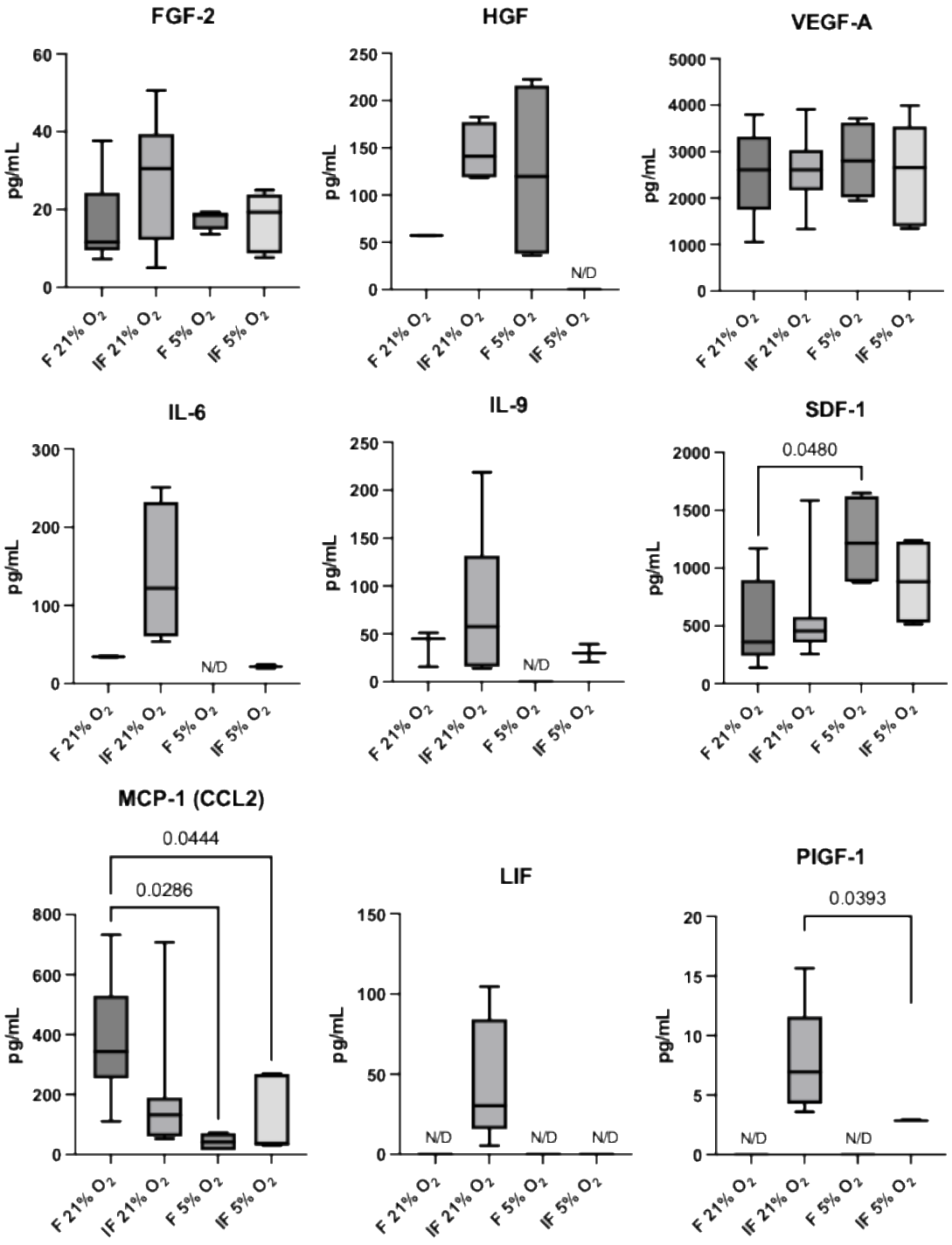


Figure 5. Secretome profile of F and IF MenSCs cultured at 5% O_2 (F n=3; IF n=3) and 21% O_2 (F n=5; IF n=8). Cytokines, chemokines and growth factors were quantified in conditioned media using a multiplex Luminex assay. Biological sample numbers vary by analyte (n=3-8, depending on group) according to sample availability and reliable detection. Statistical comparisons are indicated in the individual panels.

3.2.5. MenSC proteomic remodeling by oxygen tension and fertility status

Cellular proteomic profiles were remodeled by oxygen tension, and the direction and magnitude of this remodeling differed between F and IF donor-derived MenSCs (Fig. 6, Fig. 7, Fig. 8). In F MenSCs, 5% O_2 was associated with increase of metabolism regulator ACO1 (Aconitase 1) and protein synthesis-related protein FARSB (Phenylalanyl-tRNA synthetase subunit beta), whereas secreted GREM1 (Gremlin-1) and ECM/cytoskeletal-related protein FGD4 (FYVE, RhoGEF and PH domain containing 4) were relatively higher at 21% O_2.

14

ACO1, also known as Iron Regulatory Protein 1 (IRP1), is a bifunctional cytosolic protein that switches between an iron-dependent metabolic enzyme and an RNA-binding regulator of iron homeostasis, while FARSB (Phenylalanyl-tRNA synthetase subunit beta) gene encodes the beta subunit of the cytoplasmic enzyme phenylalanyl-tRNA synthetase (PheRS) (21). The increase of these factors is consistent with increased glycolysis and proliferation in F MenSCs cultured at 5% O_2 compared with those cultured at 21% O_2.

GREM1 is produced by specific cells—such as stromal fibroblasts and skeletal stem cells—that primarily blocks bone morphogenetic protein (BMP) signaling in neighboring cells), while FGD4 (also known as frabin) encodes an actin-filament binding protein that localizes to the cytoplasm, cytoskeleton, and filopodia to regulate cell shape, migration, and adhesion (22)(23). Therefore, the increased levels of GREM1 and FGD4 in F MenSCs at 21% O_2 compared to 5% O_2 is consistent with oxygen-dependent remodeling of stromal/cytoskeletal processes.

IF cells showed a distinct response, with signaling- and chromatin-associated candidates such as PTPN13 (Protein Tyrosine Phosphatase Non-Receptor Type 13) and GSK3B **(**Glycogen Synthase Kinase 3 Beta) increased at 5% O_2, and metabolism/redox-associated candidates such as PLIN2 (Perelipin 2) and HMOX1 (Heme Oxygenase 1) relatively higher at 21% O_2 (full candidate lists in Supplementary Table S1 and Table 1). PTPN13 is a non-receptor protein tyrosine phosphatase involved in the regulation of multiple cellular signaling processes, including cell adhesion and cytoskeletal organization (24), whereas GSK3B is a multifunctional serine/threonine kinase involved in pathways regulating metabolism, proliferation and cell-fate decisions. Their increased abundance in IF MenSCs at 5% O_2 therefore indicates oxygen-dependent remodeling of intracellular signaling in these cells. Given the exploratory nature of the cellular proteomic analysis, the potential relationship of these changes to endometrial function and infertility requires further functional validation.

On the other hand, PLIN2 is an essential structural coat protein found on the surface of intracellular lipid droplets (LDs), playing a critical role in lipid accumulation, storage stabilization, and cellular metabolic switches, while HMOX1 plays a critical cytoprotective, anti-inflammatory, and antioxidant role in mesenchymal stem/stromal cells (MSCs) (25). The upregulation of PLIN2 and HMOX1 in IF MenSCs at 21 % O_2 can be related to the IF cell metabolic changes protecting cells against oxygen tension.

Fertility comparisons also depended on oxygen condition: at 5% O_2, F MenSCs showed higher TMEM65 **(**Transmembrane Protein 65**,** a highly conserved protein localized primarily within the inner mitochondrial membrane), PXDN (Peroxidasin, an extracellular matrix (ECM) enzyme), SGCB (gene**,** encoding beta-sarcoglycan**)**, SLC44A2 (Solute Carrier Family 44 Member 2, also known as Choline Transporter-Like Protein 2 (CTL2), is a transmembrane protein l), MYADM (Myeloid-associated differentiation marker, a transmembrane protein) and PLXNA1 (Plexin A1) a critical transmembrane coreceptor), whereas the 21% O_2 highlighted a different set including THBS1 (Thrombospondin-1, a matricellular protein) and member of primary location-related genes (PLGs) MX1. Data show that 5% O_2 in F MenSCs upregulates many proteins related to the mitochondria metabolism and plasma membrane that regulate proliferation, migration, differentiation and tissue regeneration, while 21% O_2 strongly decreased number of these proteins. No cellular contrast produced a broad set of FDR-significant individual proteins, therefore, these candidates are interpreted primarily at pathway level.

15

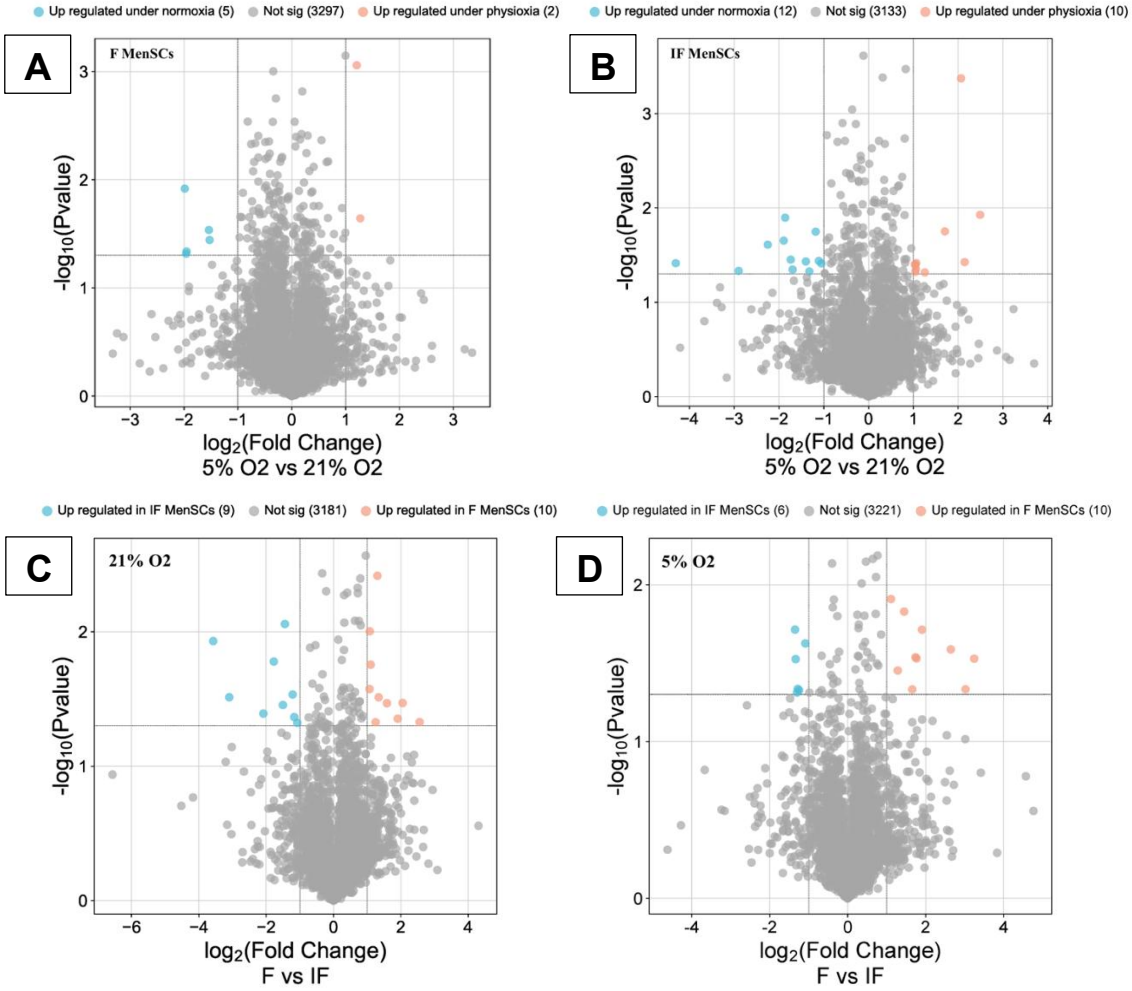


Figure 6. Cellular proteomic changes in MenSCs according to oxygen tension and fertility status. Volcano plots show (A) fertile (F) MenSCs, 5% O_2 vs 21% O_2; (B) infertile (IF) MenSCs, 5% O_2 vs 21% O_2; (C) fertile vs infertile (F vs IF) MenSCs at 21% O_2; and (D) fertile vs infertile (F vs IF) MenSCs at 5% O_2. The x-axis represents $\log_2$ fold change and the y-axis $-\log_{10}(p)$. Highlighted proteins meet the exploratory volcano criterion of nominal $p<0.05$ and $|\log_2 FC|\geq 1$. Technical MS replicates were averaged before donor-level statistical testing.

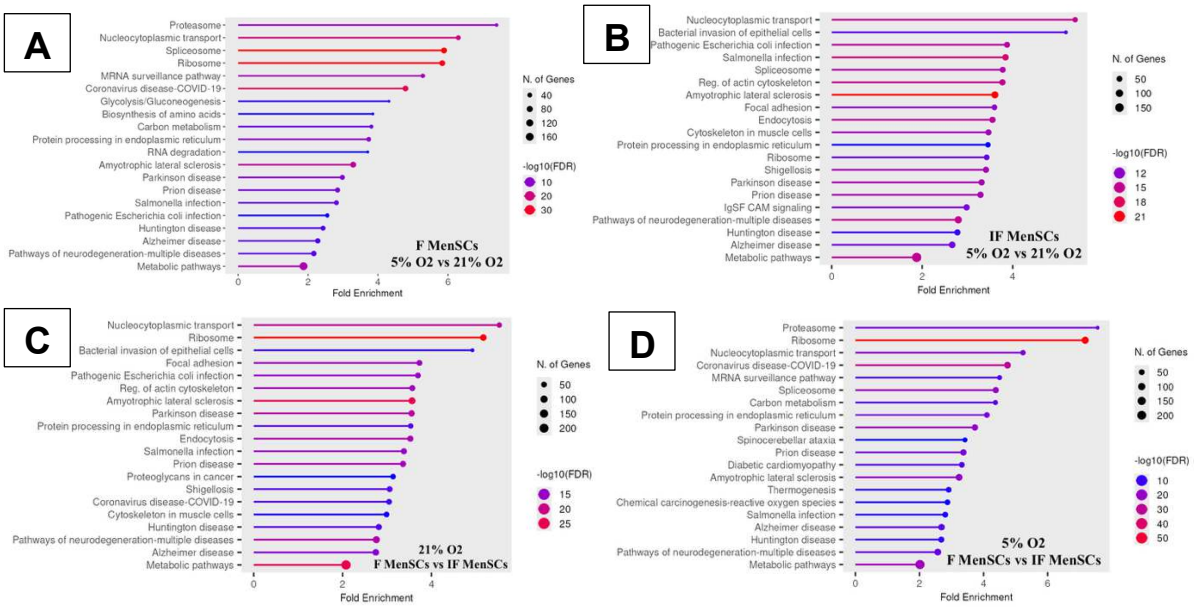


Figure 7. Functional enrichment of cellular proteomic changes. KEGG/pathway schemes show (A) fertile (F) MenSCs, 5% O_2 vs 21% O_2; (B) infertile (IF) MenSCs, 5% O_2 vs 21% O_2; (C) fertile vs infertile (F vs IF) MenSCs at 21% O_2; and (D) fertile vs infertile (F vs IF) MenSCs at 5% O_2. KEGG/pathway enrichment was generated from oxygen-

16

responsive proteins in F and IF MenSCs using ShinyGO (version 0.86.0). Dot size indicates the number of genes represented in each term and color represents enrichment significance as shown in the plot legend.

Pathway enrichment supported the single-protein observations and emphasized oxygen-sensitive processes involving metabolism, ribosomal/protein processing, cytoskeletal organization, signaling and stress adaptation. Importantly, pathway profiles differed between F and IF MenSCs, consistent with the hypothesis that fertility status modifies the biological response to oxygen tension.

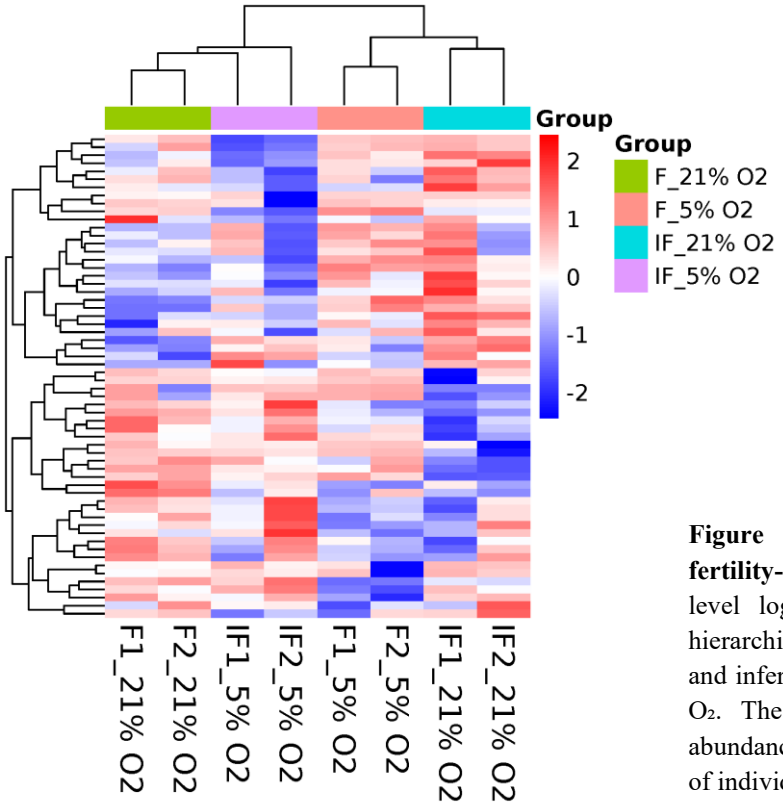


Figure 8. Heatmap of selected oxygen- and fertility-associated proteins in MenSCs. Donor-level log_2 LFQ intensities were row-scaled and hierarchically clustered. Columns represent fertile (F) and infertile (IF) MenSCs cultured at 5% O_2 or 21% O_2. The heatmap illustrates coordinated protein-abundance patterns rather than independent validation of individual biomarkers.

3.2.6. MenSC-EV proteomic remodeling by oxygen tension and fertility status

MenSC-EVs have been characterized according to international EV guidelines in our previous studies and have shown both biomarker and functional potential (4)(5).

EV proteomics demonstrated that oxygen tension remodels not only the intracellular MenSCs proteome but also the protein cargo exported in EVs, and that this response is modified by fertility status (Fig. 9, Fig. 10, Fig. 11). In F MenSC-EVs, 5% O_2 was associated with higher RNA/protein-processing and Ca^{2+}-handling candidates such as HNRNPH1/HNRNPH2 (Heterogeneous Nuclear Ribonucleoprotein H1, and HNRNPH2 stands for Heterogeneous Nuclear Ribonucleoprotein H2) and ATP2A2 (ATPase sarcoplasmic/endoplasmic reticulum Ca2+ transporting 2), whereas ECM/growth-factor-associated candidates such as NID1 (nidogen 1) and IGFBP7 (insulin-like growth factor-binding protein 7) were relatively higher at 21% O_2. In IF MenSC-EVs, the 5% O_2-upregulated set was narrower and centered on mitochondrial/metabolic candidates such as MDH2 (malate dehydrogenase 2) and IDH2 (isocitrate dehydrogenase 2 (NADP+), whereas 21% O_2 was associated with higher redox- and receptor-signaling candidates such as TXNRD1 (thioredoxin reductase 1) and PDGFRB (platelet-derived growth factor receptor beta) (full candidate lists in supplementary Table S1 and Table 1). Fertility-associated EV differences were more prominent at

17

5% O_2 than at 21% O_2, while CD99 represented the strongest FDR-supported fertility-associated EV difference at 21% O_2 in the cleaned donor-level analysis.

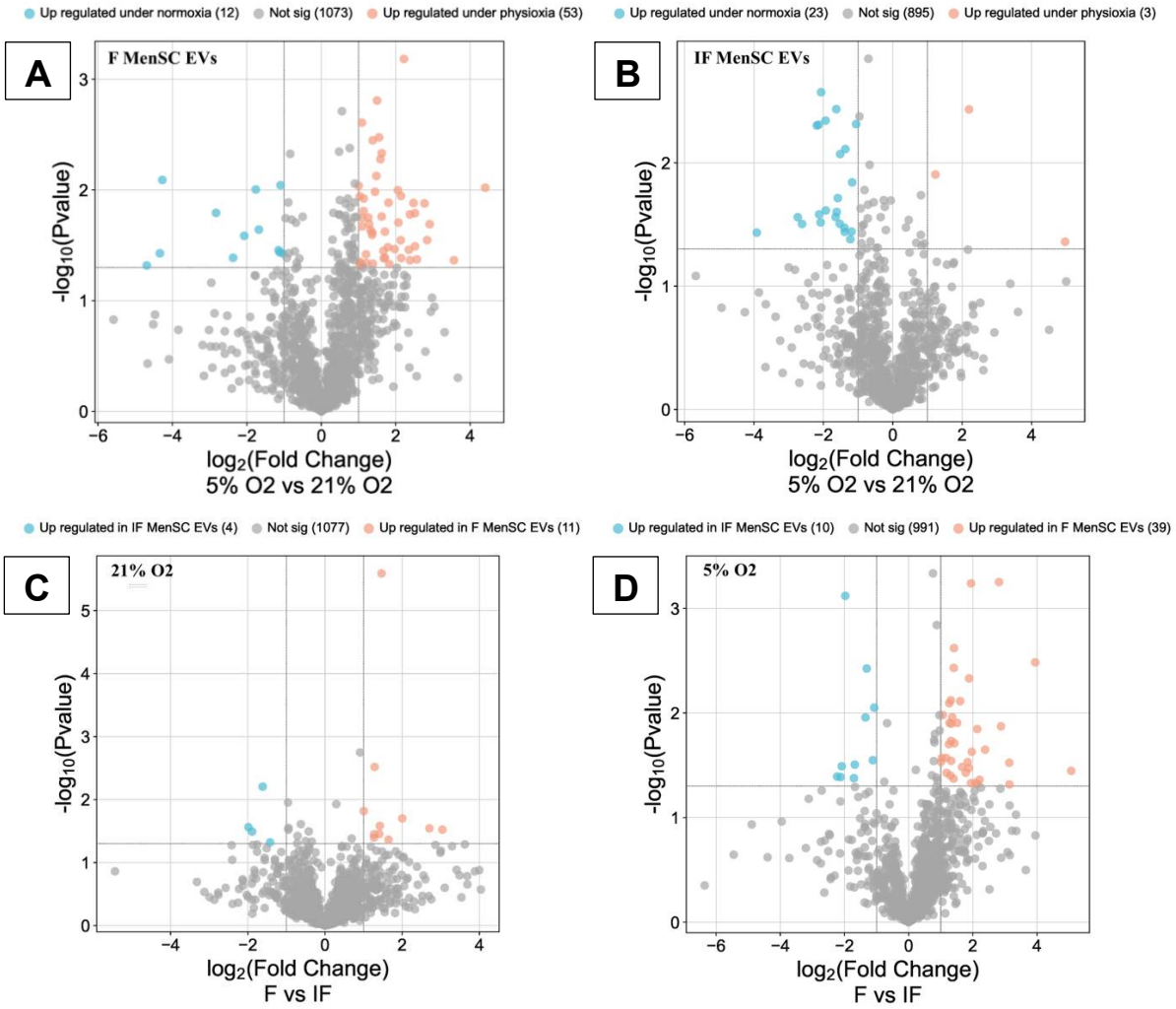
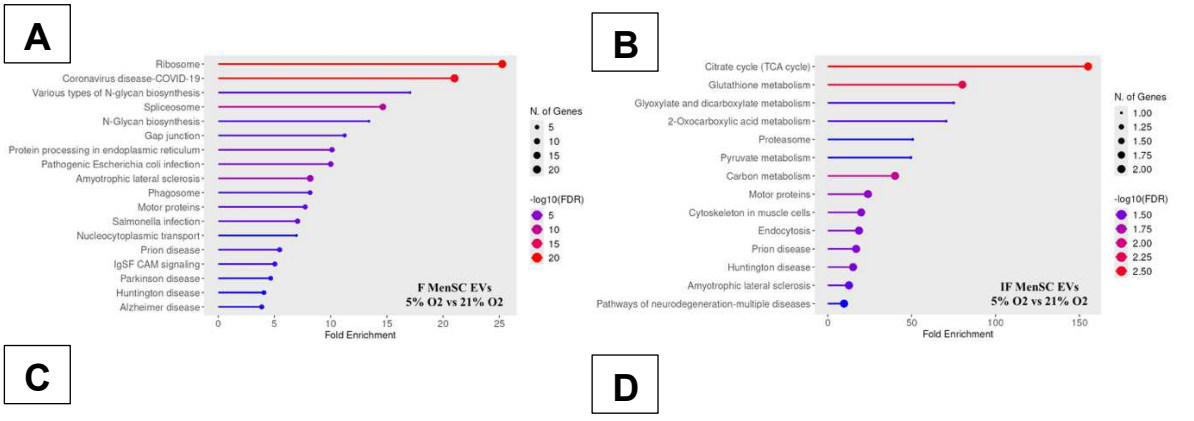


Figure 9. Proteomic changes in MenSC-derived EVs according to oxygen tension and fertility status. Volcano plots show (A) fertile (F) MenSC-EVs, 5% O_2 vs 21% O_2; (B) infertile (IF) MenSC-EVs, 5% O_2 vs 21% O_2; (C) fertile vs infertile (F vs IF) MenSC-EVs at 21% O_2; and (D) fertile vs infertile (F vs IF) MenSC-EVs at 5% O_2. Positive $\log_2$ fold change denotes higher abundance in the first group/condition named in each comparison. Highlighted proteins meet the exploratory criterion nominal $p<0.05$ and $|\log_2 FC| \geq 1$.



18

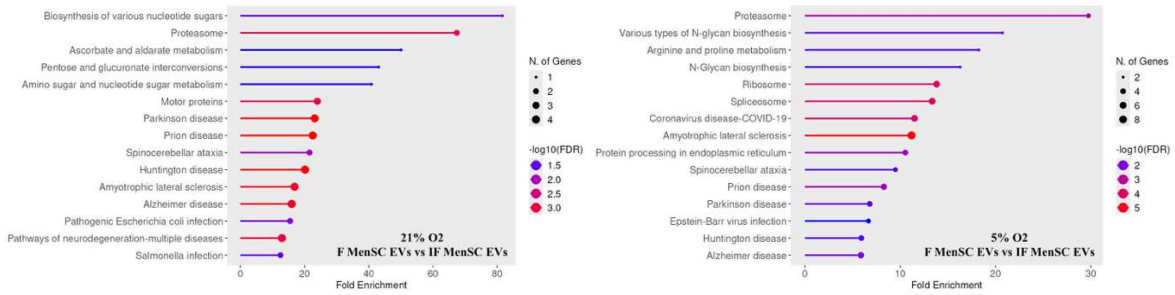


Figure 10. Functional enrichment of MenSC-EV proteomic changes. KEGG/GO enrichment analyses are shown for oxygen-response and fertility-status comparisons. Dot size indicates the number of genes represented in the pathway and color denotes enrichment significance according to the plot legend.

EV pathway enrichment showed that the exported proteome captured oxygen-dependent changes in processes related to ribosomal/RNA biology, protein processing, metabolism, vesicle/membrane organization, redox regulation and signaling. The F and IF EV pathway profiles were not identical, supporting selective cargo remodeling rather than passive reflection of the cellular proteome.

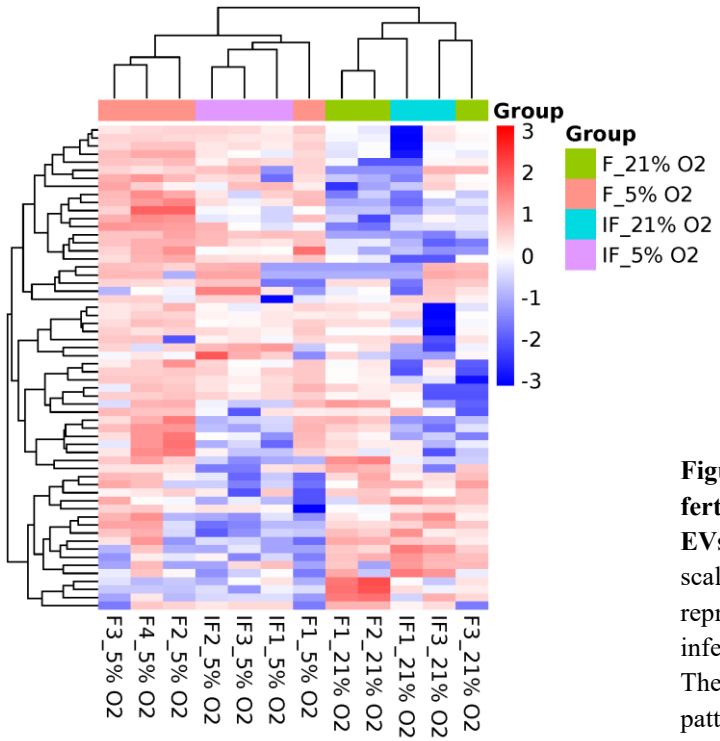


Figure 11. Heatmap of selected oxygen- and fertility-associated proteins in MenSC-derived EVs. Donor-level $\log_2$ LFQ intensities were row-scaled and hierarchically clustered. Columns represent EV samples derived from fertile (F) and infertile (IF) MenSCs cultured at 5% O_2 or 21% O_2. The heatmap visualizes coordinated EV-cargo patterns across donors and conditions.

3.2.7. Integrated cellular and EV proteomic responses

Integrated analysis demonstrated that cellular and EV proteomic responses were more coherent at the pathway level than at the level of identical individual proteins (Table 1 and supplementary Table 1).

Metabolic/redox remodeling-related proteins: Cell-associated were ACO1 (Aconitase 1), PLIN2 (Perilipin-2), PC (phosphatidylcholine) and HMOX1 (heme oxygenase 1). EVs-associated - MDH2 (malate dehydrogenase 2), IDH2 (isocitrate dehydrogenase [NADP(+)] 2), TXN (Thioredoxin), TXNRD1 (thioredoxin reductase 1) and TFRC (transferrin receptor).

19

Ca^{2+}-related regulation linked: Cell-associated - PPP3CB (protein phosphatase 3 catalytic subunit beta). EVs-associated - ATP2A2 (ATPase sarcoplasmic/endoplasmic reticulum Ca2+ transporting 2) and AHNAK (neuroblast differentiation-associated protein AHNAK (also known as AHNAK nucleoprotein or desmoyokin)).

ECM/cytoskeletal remodeling connected: Cell-associated - GREM1 (Gremlin 1, DAN family BMP antagonist), PXDN (Peroxidasin), COL6A2 (collagen type VI alpha 2 chain), THBS1 (Thrombospondin 1), FGD4 gene (also called Frabin) encoding a protein that regulates the actin cytoskeleton and activating the small GTPase CDC42) and SMTN (smoothelin). EVs-associated - GREM1 (Gremlin 1, DAN family BMP antagonist), PLOD1 (Procollagen-Lysine,2-Oxoglutarate 5-Dioxygenase), PLEC (Plecostomus), NID1 (Nidogen 1) and MYH10 (myosin heavy chain 10).

Growth and migration signaling connected: Cell-associated - GRB2 (Growth factor receptor-bound protein 2), FGD4 (FYVE, RhoGEF and PH domain-containing protein 4), GSK3B (glycogen synthase kinase 3 beta), PTPN13 (Protein tyrosine phosphatase non-receptor type 13). EVs-associated - PDGFRB (platelet-derived growth factor receptor beta), RRAS2 (Ras-related protein R-Ras2), NRAS (neuroblastoma RAS viral oncogene homolog) and LRP1 (Low-density lipoprotein receptor-related protein 1). GREM1 was notable because oxygen-associated changes were detected in both cellular and EV datasets.

Despite this pathway-level convergence, direct correspondence between cellular and EV proteins was limited. This is consistent with selective EV cargo incorporation and indicates that EV composition does not simply reproduce the intracellular proteome. Collectively, the integrated analysis supports coordinated remodeling of cellular state and exported EV cargo by oxygen tension, with the pattern of this response differing according to fertility status.

Table 1. Comparison of proteomic signatures of MenSCs and their secreted EVs, according to fertility-state and oxygen tension.

Biological process	*Compartment*	*F response*	*IF response*	*Fertility-associated differences*
Metabolism / redox	MenSC	5% O_2: ↑ ACO1; oxygen-dependent changes in BCKDHB, ATPIF1, TMEM65	21% O_2: ↑ PLIN2, PC, HMOX1	At 5% O_2, TMEM65 ↑ in F; additional O_2 × fertility interactions
	EV	—	5% O_2: ↑ MDH2, IDH2; 21% O_2: ↑ TXN, TXNRD1, TFRC	Distinct mitochondrial/redox EV response in IF
Ca^{2+} regulation	MenSC	—	—	PPP3CB showed O_2 × fertility interaction
	EV	5% O_2: ↑ ATP2A2	21% O_2: ↑ AHNAK	Fertility-dependent Ca^{2+}-associated EV remodeling
ECM / stromal remodeling	MenSC	21% O_2: ↑ GREM1	21% O_2: ↑ COL6A2	At 5% O_2, PXDN ↑ in F; at 21% O_2, THBS1 ↑ in F
	EV	21% O_2: ↑ GREM1, NID1, IGFBP7	—	At 5% O_2, PLOD1 and PLEC ↑ in F
Cytoskeleton / migration / signaling	MenSC	21% O_2: ↑ FGD4	5% O_2: ↑ SMTN; 21% O_2: ↑ GRB2	Differential oxygen-dependent cytoskeletal response
	EV	—	21% O_2: ↑ RRAS2, CTNND1, PDGFRB, LRP1	Fertility-associated remodeling of adhesion and growth signaling
RNA / protein processing	MenSC	5% O_2: ↑ FARSB	—	Predominantly associated with F response

20

	EV	5% O_2: ↑ HNRNPH1, HNRNPH2, SRSF7, PDIA4	—	Stronger RNA/protein-processing response in F EVs
EV / membrane trafficking	EV	—	5% O_2: ↑ ARF4	At 5% O_2, LMAN2 ↑ in F; EHD1 oxygen-responsive
Immune / inflammatory signaling	MenSC/EV	—	—	MX1 differed at 21% O_2; EV CD276 showed O_2 × fertility interaction; CD99 ↑ in F EVs at 21% O_2*

4. Discussion

The present study demonstrates that oxygen tension is an important determinant of MenSCs biology, affecting cellular metabolism, oxidative status, cell-cycle distribution, surface phenotype, paracrine activity and EV protein cargo. Importantly, F and IF MenSCs did not respond identically to changes in oxygen tension. Instead, some fertility-associated differences became more apparent under physioxia (5% O_2), whereas others were more pronounced under conventional atmospheric oxygen (21% O_2). These findings indicate that oxygen tension should be considered not only as a technical culture parameter but as an environmental factor capable of modifying the phenotype through which fertility-associated differences are observed.

The functional experiments performed in F MenSCs demonstrated that culture at 5% O_2 was well tolerated and induced a pronounced metabolic adaptation. Cell viability remained high, while metabolic activity/proliferation, basal glycolysis, glycolysis and glycolytic capacity were significantly increased compared with 21% O_2. These findings are consistent with previous studies demonstrating that reduced oxygen conditions can support MSC proliferation and favor glycolysis-based energy metabolism compared with conventional atmospheric oxygen culture (26).

In contrast, holographic analysis suggested lower migration and motility following prior culture at 5% O_2. Because this analysis included only two biological donors and subsequent imaging was performed at 21% O_2, these observations should be regarded as preliminary and do not establish a direct inhibitory effect of physioxia on MenSC migration. Nevertheless, the contrasting metabolic and migratory observations suggest that reduced oxygen does not uniformly enhance all MenSC functions but instead induces a function-specific adaptive response. Such findings are important because 21% O_2 represents a relatively hyperoxic environment for many stromal-cell populations and is therefore not necessarily a biologically neutral reference condition.

Oxidative stress represented another clear oxygen-sensitive component of the MenSCs phenotype. Under 21% O_2, IF MenSCs displayed substantially higher intracellular ROS levels than F MenSCs, indicating a fertility-associated redox imbalance. However, exposure to 5% O_2 significantly reduced ROS in both groups, with a particularly pronounced reduction in IF cells, thereby attenuating the difference between F and IF MenSCs. This finding is important because it demonstrates that the fertility-associated phenotype was, in this case, more clearly expressed under atmospheric oxygen than under physioxia. Consistent with our findings, Boregowda et al. demonstrated that MSCs culture at 21% O_2 increased intracellular and mitochondrial ROS compared with 5% O_2 and activated oxidative-stress and p53-dependent responses (26). At the molecular level, changes in HMOX1, PLIN2 and PC in cells and TXN, TXNRD1, TFRC, IDH2 and MDH2 in EVs further support the involvement of redox and metabolic regulation. These observations are also consistent with our previous proteomic studies identifying oxidative-stress- and metabolism-

associated alterations in menstrual blood and MenSC-related samples from women with unexplained IF.

The dependence of the F–IF phenotype on oxygen conditions was also evident from cell-cycle analysis. Physioxia markedly increased the proportion of F MenSCs in G2M, whereas IF MenSCs showed a significant increase in S phase. Moreover, direct F–IF comparison revealed a higher G2M population in IF MenSCs at 21% O_2, while the relationship was reversed at 5% O_2, with a lower G2M population in IF than in F cells. These results suggest that F and IF MenSCs differ not simply in baseline proliferation but in the way their cell-cycle machinery adapts to oxygen availability. Interaction-associated proteins involved in mitochondrial function, transcription and chromatin regulation, including TMEM65, TOP2B and ACTL6A, provide additional molecular context for this observation, although mechanistic studies will be required to determine their direct involvement.

The surface phenotype followed a similar pattern of oxygen-dependent remodeling. MenSCs maintained their overall mesenchymal stromal phenotype under both oxygen conditions, indicating that the observed differences represented phenotypic modulation rather than loss of cellular identity. In F MenSCs, CD9 and CD105 were significantly increased under 5% O_2, whereas CD73 was higher at 21% O_2. IF MenSCs showed a more limited oxygen-dependent response, with only CD9 significantly increased under physioxia. Interestingly, our previous study of menstrual serum-derived EVs showed a nonsignificant tendency toward higher CD9 levels in EVs from F compared with IF women (5). Although these findings involve different biological compartments and experimental conditions, they suggest a potentially consistent fertility-associated pattern of CD9 regulation that warrants further investigation.

Furthermore, the main F–IF difference also depended on oxygen: CD13 was higher in IF MenSCs at 21% O_2, whereas under 5% O_2, CD105 was significantly higher in F cells. Thus, neither oxygen condition universally maximized F–IF differences; instead, different phenotypic characteristics emerged depending on the cellular environment. Such plasticity is consistent with previous studies of menstrual- and endometrial-derived stromal cells. Skliutė and colleagues have highlighted the biological plasticity of menstrual blood-derived endometrial stromal cells and their relevance for studying female infertility (27). Furthermore, studies by Skliutė, Baušytė, Ramašauskaitė and Navakauskienė demonstrated molecular and epigenetic alterations in the endometrium of women with infertility, involving processes associated with implantation, inflammation, angiogenesis and decidualization (28). Together with our findings, these observations support the concept that reproductive dysfunction is associated with changes in endometrial and MenSCs molecular states and that the expression of these differences may depend strongly on the surrounding microenvironment.

Oxygen-dependent remodeling was also evident in the soluble secretome. Most measured growth factors and cytokines, including FGF-2, HGF, VEGF-A, IL-6 and IL-9, did not show significant quantitative differences between the major experimental groups. However, SDF-1 increased significantly in F MenSCs under 5% O_2, whereas MCP-1 decreased under physioxia in both F and IF cells. Interestingly, IL-6, LIF and PlGF-1 were detectably present in IF MenSC-conditioned medium specifically under 21% O_2, whereas the other groups showed only trace or undetectable levels. Although these low-abundance findings should be interpreted cautiously, together with the ROS data they suggest that atmospheric oxygen may accentuate selected inflammatory or stress-associated features of IF MenSCs. Overall, the secretome findings therefore support selective remodeling of the paracrine state rather than a generalized increase or suppression of cytokine secretion.

22

A particularly important finding of the present study was the extensive remodeling of MenSC-derived EV cargo. EV composition is known to depend on the physiological state and environmental conditions of the parental cell, and EV cargo does not necessarily reproduce the intracellular proteome because proteins and other molecules can be selectively incorporated into EVs. Importantly, de Pedro et al. directly demonstrated that oxygen-based preconditioning of MenSCs modifies their EV proteome, with physioxia-associated EV cargo enriched in functions related to tissue regeneration, angiogenesis and immunomodulation (8). Their observation that EV cargo changed even without major alterations in EV morphology, size or number further supports the use of EV composition as a sensitive indicator of the cellular response to environmental conditions.

In the present study, EV proteomics revealed substantially more oxygen- and fertility-associated differences than the cellular proteome. F MenSC-EVs showed pronounced oxygen-dependent changes involving RNA-processing and protein-handling proteins such as HNRNPH1, HNRNPH2, SRSF7 and PDIA4, together with the Ca^{2+}-regulatory protein ATP2A2. The response of IF MenSC-EVs was different and included mitochondrial and redox-associated proteins such as MDH2, IDH2, TXN and TXNRD1. Moreover, substantially more F–IF differences were detected in EVs at 5% O_2 than at 21% O_2. These findings suggest that oxygen adaptation affects not only the intracellular proteome but also the selection of proteins incorporated into EVs, and that this process may differ according to fertility status.

The greater number of differences detected in EVs than in parental cells is particularly interesting from a biomarker perspective. Selective EV packaging may concentrate molecular changes that are relatively subtle in whole-cell proteomes, potentially providing a more sensitive representation of the physiological or pathological state of the parental cell. EVs derived from the reproductive tract have increasingly been investigated as biomarkers of endometrial receptivity, implantation and reproductive disorders, and proteomic studies have identified EV proteins related to adhesion, extracellular-matrix organization, oxidative regulation and embryo–maternal communication (29)(30). Notably, the EV proteomic analysis also drew on a larger donor cohort than the cellular proteomic dataset, which adds statistical confidence to these EV-associated differences and is consistent with selective EV cargo packaging concentrating oxygen- and fertility-associated signals that are subtler at the whole-cell level. The present results support MenSC-EVs as a promising source of candidate molecular signatures capable of distinguishing F and IF phenotypes. These findings position MenSC-EV cargo as a promising source of candidate molecular signatures, with confirmation in larger independent cohorts as the natural next step toward clinical application.

Importantly, direct correspondence between cellular and EV proteins was limited, which is expected because EV cargo is selectively packaged. Nevertheless, several biologically coherent cross-compartment relationships were observed. GREM1 showed oxygen-associated changes in both cells and EVs, while cellular and EV proteins collectively converged on mitochondrial metabolism and redox regulation, Ca^{2+} homeostasis, cytoskeletal organization, growth-factor signaling and ECM remodeling. These pathway-level relationships may be more informative than direct one-to-one protein overlap and suggest that EVs capture broader aspects of the oxygen-dependent cellular state.

Overall, our findings demonstrate that oxygen tension actively influences MenSC metabolism, redox balance, cell-cycle progression, surface phenotype, secretory activity and EV cargo. Importantly, F and IF MenSCs do not respond identically to this environmental cue. Some fertility-associated differences, particularly the elevated ROS phenotype of IF cells, were more pronounced at conventional 21% O_2, whereas other differences emerged or became stronger at 5% O_2. Thus, oxygen conditions can influence which fertility-associated MenSC characteristics are

23

experimentally detected. EV cargo showed particularly extensive oxygen- and fertility-associated remodeling and, together with the pathway-level convergence observed between cellular and EV proteomes, supports further investigation of MenSC-EVs as a source of molecular signatures associated with fertility status and oxygen adaptation.

5. Conclusions

This study demonstrates that oxygen tension is an important determinant of MenSC phenotype and that oxygen-dependent adaptation differs according to fertility status. Culture at 5% O_2 altered MenSC metabolism, redox state, cell-cycle distribution, surface phenotype and secretory activity, while the direction and magnitude of several responses differed between F and IF MenSCs. Importantly, some fertility-associated differences were more evident at 5% O_2, whereas others were more pronounced under conventional 21% O_2, demonstrating that culture oxygen can influence how fertility-associated MenSC phenotypes are detected.

EV cargo showed extensive oxygen- and fertility-associated remodeling and provided a particularly informative molecular readout of MenSC adaptation. These findings support MenSC-EVs as a promising source of candidate fertility-associated molecular signatures, although validation in larger independent cohorts is required before their biomarker potential can be established.

The present study has several limitations. The F and IF donor definitions are inherently confounded with parity and, to a lesser extent, age: F participants were defined in part by prior live birth, whereas IF participants had not conceived, and the two groups had overlapping but not identical age ranges (27–40 vs 32–42 years). These factors could not be fully disentangled from fertility status in the present cohort and should be considered when interpreting group differences. In addition, all donors were recruited from a single center in Lithuania, which may limit generalizability to other populations. Sample sizes varied by assay in line with the exploratory, hypothesis-generating stages of this study: the cellular proteomic analysis (two F and two IF biological donors) is best interpreted through convergent pathway-level patterns rather than individual protein-level significance after multiple-testing correction, and the holographic migration data (n = 2) should likewise be read as a preliminary observation. The EV proteomic analysis, which included a larger donor cohort, provided stronger statistical support and is a natural focus for confirmation in future, larger-cohort studies. Finally, 5% O_2 should be regarded as a physiologically relevant culture condition rather than an exact representation of the oxygen concentration experienced by MenSCs within the endometrium in vivo.

6. List of abbreviations

2-DG, 2-deoxy-D-glucose; ANOVA, analysis of variance; BMP, bone morphogenetic protein; BSA, bovine serum albumin; CD, cluster of differentiation; CO_2, carbon dioxide; CXCL12, C-X-C motif chemokine ligand 12; CXCR4, C-X-C motif chemokine receptor 4; DAPI, 4′,6-diamidino-2-phenylindole; DMEM/F12, Dulbecco's Modified Eagle Medium/Nutrient Mixture F-12; ECAR, extracellular acidification rate; ECM, extracellular matrix; ER, endoplasmic reticulum; EV, extracellular vesicle; F, fertile; FBS, fetal bovine serum; FDR, false discovery rate; FGF-2, fibroblast growth factor 2; FITC, fluorescein isothiocyanate; GO, Gene Ontology; HGF, hepatocyte growth factor; IF, unexplained infertility/infertile group; IL, interleukin; KEGG, Kyoto Encyclopedia of Genes and Genomes; LFQ, label-free quantification; LIF, leukemia inhibitory factor; MCP-1, monocyte chemoattractant protein-1; MenSC, menstrual blood-derived mesenchymal stromal cell;

MFI, median fluorescence intensity; MISEV, Minimal Information for Studies of Extracellular Vesicles; MS, mass spectrometry; O_2, oxygen; PBS, phosphate-buffered saline; PE, phycoerythrin; PlGF-1, placental growth factor 1; PS, penicillin/streptomycin; ROS, reactive oxygen species; SD, standard deviation; SDF-1, stromal cell-derived factor 1; TGF-β, transforming growth factor beta; VEGF-A, vascular endothelial growth factor A; uIF, unexplained infertility.

7. Declarations

Ethical statement

Menstrual blood collection and use of donor-derived cells were performed in accordance with the Lithuanian Bioethical laws and applicable institutional guidelines. The donor framework used in the related MenSC studies was approved by the Vilnius Regional Biomedical Research Ethics Committee under permission No. 158200-14-741-257 (title: “Characterization of stem and/or higher differentiation cells, derived from tissues remaining after surgical interventions, and in vitro evaluation of their ability to restore damaged tissues or to induce their regeneration", Dates of approval: 2014 06 10; Date of extension: 2025 07 23; Due date after extension: 2030 07) and No. 2021/6-1363-837 (title: “Imaging and analysis of pathophysiological cellular and extracellular matrix biomarkers in various tissues using innovative combined detection methods", Dates of approval: 2021 06 23; Due date: 2031 07) and its approved amendments. Written informed consent was obtained from all participants before sample collection.

Consent for publication

Not applicable.

Availability of data and materials

The proteomics datasets generated and analysed during the current study are provided as supplementary materials.

Competing interests

The authors declare that they have no competing interests.

Funding

The project was funded by the European Social Funds and Lithuanian Research Council, according to the activity EP PerMed, NR. No 2021/695 „Personalisation of Treatment for Female Infertility and Recurrent Pregnancy Loss of Unknown Etiology”, acronym: “Perfert“.

Author contribution

I.U. – conceptualization, methodology, investigation, data interpretation, visualization, writing – original draft, writing - review and editing, supervision; J.P. and R.V. - MenSC/EV experiments, including surface markers, cell cycle, proteomics, investigation, data interpretation,

review and editing; and D.B. – MenSCs experiments, including ROS, review and editing; K.G., A.O. – cellular assays, writing original draft and data interpretation; R.N. and V.B. – writing/review and editing, supervision; K.B. and M.M. – proteomic/bioinformatics interpretation and critical review; L.P. and Z.K. – participant/sample support and clinical contribution; E.B. – conceptualization, supervision, methodology, critical review and editing.

Acknowledgements

The authors thank all study participants and the clinical and technical staff who contributed to menstrual blood collection, cell culture, flow-cytometry, proteomic and bioinformatic analyses.

Also, the authors want to acknowledge Lithuanian Research Council and European Social Funds for providing funds for this project.

Generative AI statement

During the preparation of this manuscript, the authors used AI tools to assist with language editing and grammar refinement of the final manuscript draft. All scientific interpretation, critical evaluation of the literature, conclusions, figures, and final manuscript content were independently reviewed, verified, and approved by the authors, who take full responsibility for the accuracy and integrity of the work.

8. References

1. Robalo Cordeiro M, Roque R, Laranjeiro B, Carvalhos C, Figueiredo-Dias M. Menstrual Blood Stem Cells-Derived Exosomes as Promising Therapeutic Tools in Premature Ovarian Insufficiency Induced by Gonadotoxic Systemic Anticancer Treatment. Int J Mol Sci. 2024;25(15).
2. Meng X, Ichim TE, Zhong J, Rogers A, Yin Z, Jackson J, et al. Endometrial regenerative cells: a novel stem cell population. J Transl Med. 2007;5:57.
3. Alcayaga-Miranda F, Cuenca J, Luz-Crawford P, Aguila-Díaz C, Fernandez A, Figueroa FE, et al. Characterization of menstrual stem cells: angiogenic effect, migration and hematopoietic stem cell support in comparison with bone marrow mesenchymal stem cells. Stem Cell Res Ther. 2015;6:32.
4. Vaiciuleviciute R, Brennan K, Uzieliene I, Pachaleva J, Kasilovskiene Z, Piesiniene L, et al. Proteomic signature of menstrual blood mesenchymal stromal cells and their extracellular vesicles in women with unexplained infertility. Reprod Biomed Online. 2025;
5. Brennan K, Vaiciuleviciute R, Uzieliene I, Pachaleva J, Kasilovskiene Z, Piesiniene L, et al. Menstrual blood serum extracellular vesicles reveal novel molecular biomarkers and potential endotypes of unexplained infertility. 2025;1–15.
6. Chen C, Tang Q, Zhang Y, Yu M, Jing W, Tian W. Physioxia : a more effective approach for culturing human adipose-derived stem cells for cell transplantation. 2018;1–12.
7. Maybin JA, Critchley HOD. Menstrual physiology: Implications for endometrial pathology and beyond. Hum Reprod Update. 2015;21(6):748–61.
8. de Pedro MÁ, López E, González-Nuño FM, Pulido M, Álvarez V, Marchena AM, et al. Menstrual blood-derived mesenchymal stromal cells: impact of preconditioning on the cargo of extracellular vesicles as potential therapeutics. Stem Cell Res Ther. 2023;14(1):1–20.
9. Zhang HC, Liu X Bin, Huang S, Bi XY, Wang HX, Xie LX, et al. Microvesicles derived from human umbilical cord mesenchymal stem cells stimulated by hypoxia promote angiogenesis both in vitro and in vivo. Stem Cells Dev. 2012;21(18):3289–97.

26

10. Kugaudaite G, Bakutyte I, Bagdonas E, Vaiciuleviciute R. Menstrual blood-derived mesenchymal stromal cell extracellular vesicles stimulate chondrocytes and cartilage extracellular matrix synthesis in vitro. 2026;1–19.
11. Uzieliene I, Bagdonas E, Hoshi K, Sakamoto T, Hikita A, Tachtamisevaite Z, et al. Different phenotypes and chondrogenic responses of human menstrual blood and bone marrow mesenchymal stem cells to activin A and TGF-β3. Stem Cell Res Ther. 2021;12(1):1–16.
12. Uzieliene I, Urbonaite G, Tachtamisevaite Z, Mobasheri A, Bernotiene E. The potential of menstrual blood-derived mesenchymal stem cells for cartilage repair and regeneration: Novel aspects. Vol. 1, Stem Cells International. 2018. p. 1–10.
13. Duff SE, Li C, Garland JM, Kumar S. CD105 is important for angiogenesis : evidence and potential applications.
14. Andreu Z, Yáñez-mó M. Tetraspanins in extracellular vesicle formation and function. 2014;5(September):1–12.
15. ERJA KERKELA, ANITA LAITINEN, JARKKO RABINA, SAMI VALKONEN, MAARIT TAKATALO, ANTTI LARJO, JOHANNA VEIJOLA, MILLA LAMPINEN, PIA SILJANDER, PETRI LEHENKARI, KAIJA ALFTHAN SL. Adenosinergic Immunosuppression by Human Mesenchymal Stromal Cells Requires Co-Operation with T cells. 2016;781–90.
16. Yellowley C. CXCL12 / CXCR4 signaling and other recruitment and homing pathways in fracture repair. Bonekey Rep [Internet]. 2013;2(3):1–9. Available from: http://dx.doi.org/10.1038/bonekey.2013.34
17. Deshmane SL, Sergey Kremlev, 1 Shohreh Amini and BES. Monocyte Chemoattractant Protein-1 (MCP-1): An Overview. J Interf CYTOKINE Res. 2009;29(6).
18. Tanaka T, Narazaki M, Kishimoto T. IL-6 in Inflammation, Immunity, and Disease. Cold Spring Harb Perspect Biol. 2014;6(Kishimoto 1989):1–16.
19. Hiroyuki Hirai, Peter Karian and NK. Regulation of embryonic stem cell self-renewal and pluripotency by leukaemia inhibitory factor. Biochem J. 2012;438(1):11–23.
20. Nikolaos Vrachnis, Emmanouil Kalampokas, Stavros Sifakis, Nikolaos Vitoratos, Theodoros Kalampokas, Demetrios Botsis and ZI. Placental growth factor (PlGF): a key to optimizing fetal growth. J Matern Fetal Neonatal Med. 2013;7058(10):995–1002.
21. Cole P. Andersona, Lacy Shenb, Richard S. Eisensteinb and EAL. Mammalian iron metabolism and its control by iron regulatory proteins. Biochim Biophys Acta. 2013;1823(9):1468–83.
22. Wu M, Wu S, Chen W, Li Y. The roles and regulatory mechanisms of TGF- β and BMP signaling in bone and cartilage development , homeostasis and disease. 2024;(February 2023).
23. Nakanishi H, Takai Y. Frabin and other related Cdc42-specific guanine nucleotide exchange factors couple the actin cytoskeleton with the plasma membrane. 2008;12(4):1169–76.
24. Hamyeh M, Bernex F, Larive RM, Naldi A, Urbach S, Puech C, et al. Theranostics PTPN13 induces cell junction stabilization and inhibits mammary tumor invasiveness. 2020;10(3).
25. Sztalryd C, Brasaemle DL. The perilipin family of lipid droplet proteins: Gatekeepers of intracellular lipolysis. 2018;1862:1221–32.
26. SIDDARAJU V. BOREGOWDA, VEENA KRISHNAPPA, JEREMY W. CHAMBERS, PHILIP V. LOGRASSO, WEN-TZU LAI, LUIS A. ORTIZ DGP. Atmospheric Oxygen Inhibits Growth and Differentiation of Marrow-Derived Mouse Mesenchymal Stem Cells via a p53-Dependent Mechanism: Implications for Long-Term Culture Expansion. Stem Cells. 2012;975–87.
27. Skliutė G, Baušytė R, Borutinskaitė V, Valiulienė G, Kaupinis A, Valius M, et al. Menstrual blood-derived endometrial stem cells' impact for the treatment perspective of female infertility. Int J Mol Sci. 2021;22(13).
28. Baušyt R. Characterization of Epigenetic and Molecular Factors in Endometrium of Females with Infertility. 2022;
29. Rai A, Poh QH, Fatmous M, Fang H, Gurung S, Vollenhoven B, et al. Proteomic profiling of human uterine extracellular vesicles reveal dynamic regulation of key players of embryo

implantation and fertility during menstrual cycle. 2021;(October 2020):1–17.
30. Benítez MS, Cristina M, García C, Corachán A, Faus A, Pellicer A, et al. Proteomic analysis of extracellular vesicles secreted by primary human epithelial endometrial cells reveals key proteins related to embryo implantation. Reprod Biol Endocrinol [Internet]. 2022;1–16. Available from: https://doi.org/10.1186/s12958-021-00879-x

28

Supplementary Files

This is a list of supplementary files associated with this preprint. Click to download.

- Supplementarytable1.docx
- SupplementaryFile2MenSCEVphysioxiafertilityproteomics.xlsx
- Supplementaryfile1MenSCphysioxiafertilityproteomics.xlsx